Supporting Information

for

Kinetic rate constants of gold nanoparticles deposition on silicon

*Valentina Onesto[1], Francesco Gentile[2], Mario Russo[1], Marco Villani[3], Patrizio Candeloro[1], Gerardo Perozziello[1], Natalia Malara[1], Enzo Di Fabrizio[4], M Laura Coluccio[1]**

[1] Department of Experimental and Clinical Medicine. University Magna Graecia, Catanzaro, 88100, Italy

[2] Department of Electrical Engineering and Information Technology, University Federico II, 80125, Naples, Italy

[3] IMEM-CNR, Parco Area delle Scienze, 37/A 43123 Parma, Italy

[4] Physical Science & Engineering Division, King Abdullah University of Science and Technology, Thuwal, 23955-6900, Saudi Arabia

E-mail: coluccio@unicz.it

Number of Pages: 6

Number of Figures: 2

Number of Tables: 2

RESULTS AND DISCUSSION

The efficiency of the electroless deposition was valuated by a comparison of SEM images taken using different modalities of detection (NTS BSD and In Lens). In **Table SI 1** the name of each image and the characteristics of the represented sample is reported.

NTS BSD is a retractable five diode backscattered electron detector (BSD) used for qualitative compositional imaging in high vacuum. With this modality, areas of the sample with heavier elements appear brighter. Thus, NPSi NPs covered with gold are easily recognizable as those particles in the image with higher contrast respect to the background.

In Lens SE detector is a high resolution secondary electron (SE) detector that reduces the percentage of SE and SE signals observed and artefacts. With this modality, the resolution is improved, while shadow contrasts are lost making the sample look flatter than it is. It is used to image NPs regardless of their composition.

The efficiency of deposition is greater than 80% for all configuration of growth and approaches unity in all cases for deposition time greater than approximately 40 min. From the SEM images of the samples. We analysed the nano-porous silicon nanoparticles (NPSi NPs) using two different SEM modalities: (i) NTS BSD and (ii) In Lens (**Fig. SI 1** and **2**).

From the analysis of NPSi NPs imaged using either the NTS BSD and the In Lens SE modality, we determined the number of silicon particles correctly covered with metallic gold at the end of the process of electroless deposition (N_{gold}), and the total number of particles in a sample (N_{tot}). The ratio of the particles covered with gold to the total number of particles in a sample, represents the efficiency of the process η, $\eta = N_{gold}/N_{tot}$. η indicates the percentage of NPSi NPs, initially contained in the solution before the process of electroless deposition, correctly functionalized with metallic gold at the end of the process. Ratios were calculated using either the *number* of particles measured in a SEM micrograph (η_N), and the *area* of those particles derived through image analysis algorithms (η_A). Results indicate that the efficiency of the process is as high as 90% considering the number of particles in the image ($\eta_N \sim 0.9$), and is higher than 90% considering the total area of the particles ($\eta_A \sim 0.93$), for a fixed temperature $T = 50°$ and a time of deposition of $t = 24\ h$ (data from **Fig SI 1**). The same analysis repeated for different temperatures and times of the process indicates that the efficiency of the process is generally high – the lowest measured value of efficiency being $\eta_A \sim 0.81$ after 10 minutes of electroless growth at $T = 50°$ (**Tab SI 2**, data from

Fig SI 2). This, in turn, implies that the number of silicon particles left in solution (i.e., not-treated) a few minutes after the deposition is low.

Segmentation and analysis of SEM Images

SEM images were analyzed with Matlab®. Images were first converted grayscale, preprocessed to enhance contrast by contrast-limited adaptive histogram equalization (CLAHE) and low-pass filtered to remove constant power additive noise before being binarized with Otsu's method. Morphological opening was performed to remove any small white noises in the image, and morphological closing to remove any small holes in the object. Structures that were lighter than their surroundings and connected to the image border were suppressed. The images were segmented by a watershed transformation and a distance transform was used as segmentation function to split out the regions, identifying the single nanoparticles. The number of nanoparticles and their area were obtained through the regionprops function. The final area is the mean of the nanoparticle areas in the image.

Tab. SI1

Sample name	Sample characteristics
T11	Si and Au nanoparticles - T1 10min
T12	Si and Au nanoparticles - T1 60min
T13	Si and Au nanoparticles - T1 120min
T14	Si and Au nanoparticles - T1 24h
T21	Si and Au nanoparticles - T2 10min
T22	Si and Au nanoparticles - T2 60min
T23	Si and Au nanoparticles - T2 120min
T24	Si and Au nanoparticles - T2 24h

Fig. SI1

Au NP

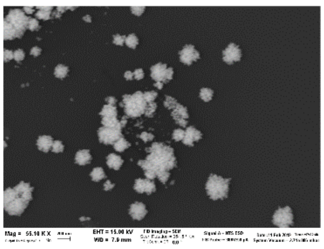

Au NP number	27
Au NP area (nm^2)	6.0453e+04

Au NP + Si NP

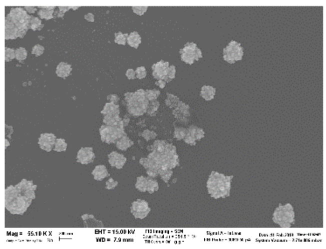

Au + Si NP number	30
Au + Si NP area (nm^2)	6.5159e+04

T24 sample
reaction time 24h
reaction temperature 50°C

$$\eta_n = \frac{N(Au)}{N(Au+Si)} = 0{,}9$$

$$\eta_A = \frac{A(Au)}{A(Au+Si)} = 0{,}93$$

Fig. SI2

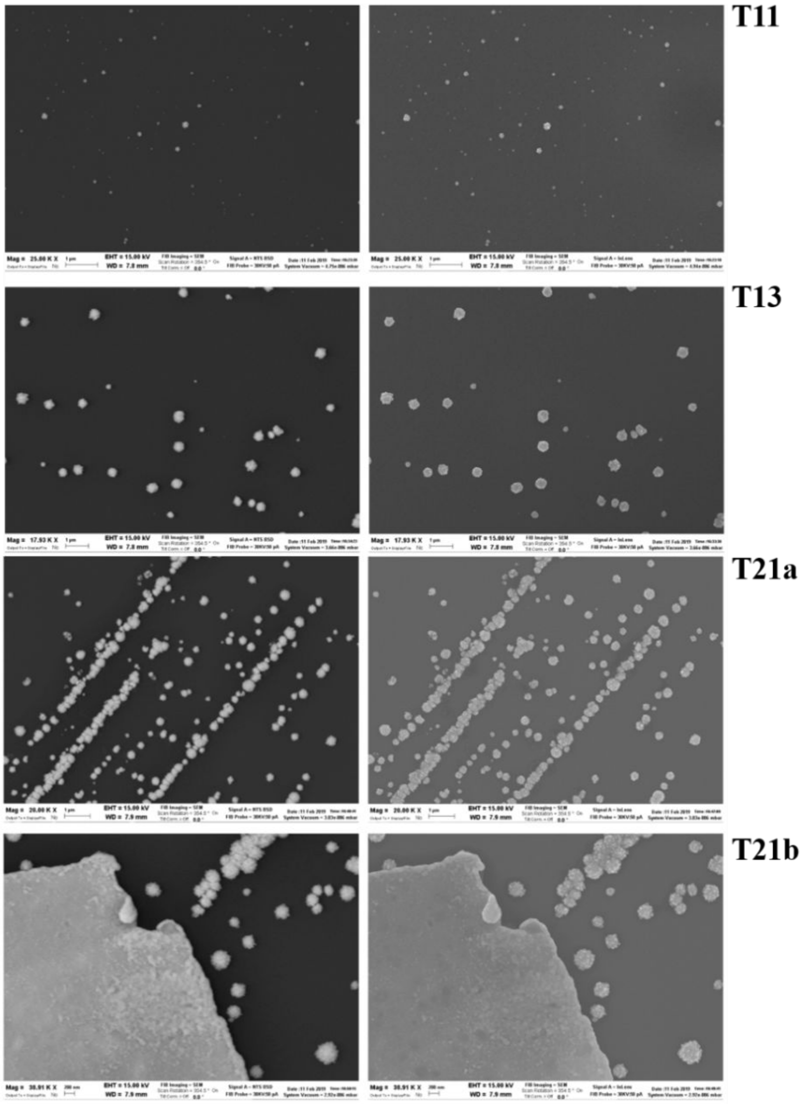

Tab. SI2

η_n –T11	0.9560
η_n –T13	0.9124
η_n –T21a	0.8670
η_n –T21b	0.8700
η_A –T11	0.8610
η_A –T13	0.9130
η_A –T21a	0.9010
η_A –T21b	0.8100